Neurobiology of Disease 167 (2022) 105669

Contents lists available at ScienceDirect

Neurobiology of Disease

journal homepage: www.elsevier.com/locate/ynbdi

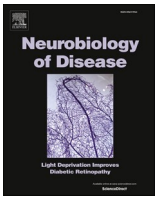

Cerebral metabolic pattern associated with progressive parkinsonism in non-human primates reveals early cortical hypometabolism

Francisco Molinet-Dronda [a,b,1], Javier Blesa [a,c,d,1], Natalia López-González del Rey [c,d,e], Carlos Juri [a,f], María Collantes [b,g], Jose A Pineda-Pardo [c,d], Inés Trigo-Damas [a,c,d], Elena Iglesias [a], Ledia F. Hernández [a,c,d], Rafael Rodríguez-Rojas [c,d], Belén Gago [a,h], Margarita Ecay [b,g], Elena Prieto [g,i], Miguel Á. García-Cabezas [e,j], Carmen Cavada [e,j], María C. Rodríguez-Oroz [a], Iván Peñuelas [b,g], José A. Obeso [a,c,d,*]

[a] Movement Disorders Laboratory, Neurosciences Area, CIMA, University of Navarra, Pamplona, Spain
[b] Translational Molecular Imaging Unit (UNIMTRA), Clínica Universidad de Navarra, IdiSNA, Pamplona, Spain
[c] Center for Networked Biomedical Research on Neurodegenerative Diseases (CIBERNED), Madrid, Spain
[d] HM CINAC (Centro Integral de Neurociencias Abarca Campal), Hospital Universitario HM Puerta del Sur, HM Hospitales, Madrid, Spain
[e] PhD Program in Neuroscience, Autónoma de Madrid University-Cajal Institute, Madrid 28029, Spain
[f] Department of Neurology, Facultad de Medicina, Pontificia Universidad Católica de Chile, Santiago, Chile
[g] Department of Nuclear Medicine, Clínica Universidad de Navarra, Pamplona, Spain
[h] Instituto de Investigación Biomédica de Málaga, Facultad de Medicina, Universidad de Málaga, Málaga, Spain
[i] Medical Physics, Clínica Universidad de Navarra, Pamplona, Spain
[j] Department of Anatomy, Histology and Neuroscience, School of Medicine, Autónoma de Madrid University, Madrid, Spain

ARTICLE INFO

Keywords:
Parkinson's disease
Positron emission tomography (PET)
[^{18}F]-fluoro-2-deoxy-D-glucose (^{18}F-FDG)
[^{11}C]-dihydrotetrabenazine (^{11}C-DTBZ)
Glucose metabolism

ABSTRACT

Dopaminergic denervation in patients with Parkinson's disease is associated with changes in brain metabolism. Cerebral *in-vivo* mapping of glucose metabolism has been studied in severe stable parkinsonian monkeys, but data on brain metabolic changes in early stages of dopaminergic depletion of this model is lacking. Here, we report cerebral metabolic changes associated with progressive nigrostriatal lesion in the pre-symptomatic and symptomatic stages of the progressive 1-methyl-4-phenyl-1,2,3,6-tetrahydropyridine (MPTP) monkey model of Parkinson's Disease. Monkeys (*Macaca fascicularis*) received MPTP injections biweekly to induce progressive grades of dopamine depletion. Monkeys were sorted according to motor scale assessments in *control*, *asymptomatic*, *recovered*, *mild*, and *severe* parkinsonian groups. Dopaminergic depletion in the striatum and cerebral metabolic patterns across groups were studied *in vivo* by positron emission tomography (PET) using monoaminergic ([^{11}C]-dihydrotetrabenazine; ^{11}C-DTBZ) and metabolic (2-[^{18}F]-fluoro-2-deoxy-D-glucose; ^{18}F-FDG) radiotracers. ^{11}C-DTBZ-PET analysis showed progressive decrease of binding potential values in the striatum of monkeys throughout MPTP administration and the development of parkinsonian signs. ^{18}F-FDG analysis in a*symptomatic* and *recovered* animals showed significant hypometabolism in temporal and parietal areas of the cerebral cortex in association with moderate dopaminergic nigrostriatal depletion. Cortical hypometabolism extended to involve a larger area in *mild* parkinsonian monkeys, which also exhibited hypermetabolism in the globus pallidum pars interna and cerebellum. In *severe* parkinsonian monkeys, cortical hypometabolism extended further to lateral-frontal cortices and hypermetabolism also ensued in the thalamus and cerebellum. Unbiased histological quantification of neurons in Brodmann's area 7 in the parietal cortex did not reveal neuron loss in parkinsonian monkeys *versus controls*. Early dopaminergic nigrostriatal depletion is associated with cortical, mainly temporo-parietal hypometabolism unrelated to neuron loss. These findings, together with recent evidence from Parkinson's Disease patients, suggest that early cortical hypometabolism may be associated and driven by subcortical changes that need to be evaluated appropriately. Altogether, these findings could be relevant when potential disease modifying therapies become available.

* Corresponding author at: Hospital HM Puerta del Sur, HM CINAC, Spain.
E-mail address: jobeso.hmcinac@hmhospitales.com (J.A. Obeso).
[1] Both authors contributed equally to this work

https://doi.org/10.1016/j.nbd.2022.105669
Received 11 November 2021; Received in revised form 7 February 2022; Accepted 21 February 2022
Available online 24 February 2022

1. Introduction

The cardinal clinical features of Parkinson's disease (PD) become apparent after extensive loss of dopaminergic neurons in the substantia nigra and dopamine in the striatum. Characterization of initial cerebral changes associated with these dopaminergic deficits is important to understand the evolution of PD (Blesa et al., 2017; Del Rey et al., 2018). In this sense, positron emission tomography (PET) imaging is routinely applied for clinical evaluation of PD patients using radioligands such as 6-[^{18}F]-fluoro-L-DOPA (^{18}F-DOPA) and [^{11}C]-dihydrotetrabenazine (^{11}C-DTBZ) for evaluating striatal dopaminergic innervation (de la Fuente-Fernandez et al., 2011; Nandhagopal et al., 2011), and 2-[^{18}F]-fluoro-2-deoxy-D-glucose (^{18}F-FDG) as a marker of cerebral glucose consumption for assessing metabolic activity (Eckert et al., 2005, 2007; Hirano et al., 2009; Huang et al., 2007; Niethammer et al., 2012).

PET studies have contributed to ascertaining the topography and evolution of dopaminergic loss in PD (de la Fuente-Fernandez et al., 2011), defining compensatory changes (Nandhagopal et al., 2011), and identifying cerebral metabolic patterns associated with motor and cognitive manifestations (Eckert et al., 2005; Hirano et al., 2009; Niethammer et al., 2012). More recently, metabolic changes in untreated, newly diagnosed PD patients studied with ^{18}F-FDG showed reduced glucose consumption in prefrontal and parietal cortices (Orso et al., 2021; Schindlbeck et al., 2019). Another study in PD patients corroborated cortical hypometabolism, as well as reduced cortico-striatal connectivity, all of which correlated with nigrostriatal dopaminergic loss (Meles et al., 2019). However, PET studies of PD patients very early at disease onset and throughout progressive evolution (Eckert et al., 2007; Huang et al., 2007) are challenging to implement and, particularly, assessing the pre-symptomatic state still proves complex.

The MPTP (1-methyl-4-phenyl-1,2,3,6-tetrahydropyridine) monkey model closely resembles pre-symptomatic and symptomatic stages of nigrostriatal neurodegeneration in PD patients. This model is an excellent tool to study early (prodromal) cerebral changes associated with parkinsonism *in vivo,* including behavior, neurophysiology and PET (Trigo-Damas et al., 2018). Metabolic changes in particular, have been well-defined in MPTP-treated parkinsonian monkeys *ex-vivo* (Mitchell et al., 1989) and *in-vivo* (Ma et al., 2012, 2015), but longitudinal studies including asymptomatic monkeys are lacking. Here, we use ^{18}F-FDG to study changes in cerebral glucose metabolism *in vivo* in MPTP monkeys in parallel with nigrostriatal depletion, including pre-symptomatic and symptomatic groups. Specifically, this study was designed to ascertain at what point of nigrostriatal dopaminergic depletion was the cortico-basal ganglia network activity impaired. In other words, to establish a threshold of dopaminergic striatal loss signaling changes beyond the nigrostriatal projection. We previously showed that around 60% striatal DA depletion signaled the onset of parkinsonism in this model (Blesa et al., 2010, 2012). We set to assess the same concept *in vivo*. In monkeys with moderate nigrostriatal lesion, the pattern of cerebral metabolism was nearly identical to what has been described in early, not-advanced PD patients. Given that MPTP intoxication does not evolve in a progressive fashion, we thought that these findings may serve to: a) Support the veracity of PET findings and correlation with early dopaminergic deficit in patients. b) Provide further insight into the mechanism leading to cortical hypometabolism.

2. Material and methods

2.1. Animals

Thirty-seven male macaque monkeys (*Macaca fascicularis*; 2.5–7.5 kg; 3 to 5 years) and sourced from R.C. Hartelust BV (Tilburg, The Netherlands), were used in this study. All animals were used in other studies and experimental conditions have been described elsewhere in greater detail (Blesa et al., 2010, 2011, 2012; Enterría-Morales et al., 2020; Jiménez-Sánchez et al., 2020; Mellone et al., 2015; Monje et al., 2020; Pifl et al., 2013, 2014, 2017). Animals were housed in an animal room under standard conditions and treated in accordance with the European and Spanish guidelines (86/609/EEC and 2003/65/EC European Council Directives; and the Spanish Government). Water and fresh fruit were available *ad libitum*. Qualified personnel health care oversaw monitoring the monkey's welfare throughout the studies. All studies were performed according to European and Spanish guidelines (86/609/EEC and 2003/65/EC European Council Directives; and Spanish Government) and were approved by the Ethical Committee for Research of the University of Navarra and Autónoma de Madrid University.

2.2. Experimental design

MPTP was given to all monkeys by systemic administration (using a dose regimen of 0.5 mg/kg i.v. every two weeks) under light anesthesia (ketamine 10 mg/kg; i.m.) as described before (Blesa et al., 2012). Motor status after injections was evaluated weekly by a validated motor score (Blesa et al., 2010, 2012). The different individual susceptibilities to MPTP were used for initial distinction and each monkey was ascribed to one specific experimental group according to the degree of motor impairment reached after MPTP administration: *asymptomatic*, *recovered*, *mild,* and *severe* parkinsonian (Blesa et al., 2012). Out of 37 monkeys, 21 monkeys were PET scanned prior to MPTP intoxication to obtain baseline (control) values for ^{11}C-DTBZ ($n = 21$) and ^{18}F-FDG ($n = 16$) (Table 1). After MPTP intoxication, one ^{18}F-FDG and one ^{11}C-DTBZ PET scans were obtained for each animal at a given motor state (see Table 1). Thus, each group is considered an independent group. In every monkey PET scans were acquired around 1 month after reaching a stable motor status (Taylor et al., 1997) and the period in-between ^{18}F-FDG and ^{11}C-DTBZ PET scans was 3–10 days. For technical reasons (PET scanning availability mainly) it was not possible to scan every animal with both radiotracers although in the majority of instances both were used (see Table 1 for number of animals, PET scans, MPTP injections, and Kurlan scores across different groups).

Animals were processed for *post-mortem* neuroanatomical and biochemical examination as described previously (Blesa et al., 2012; Enterría-Morales et al., 2020; Jiménez-Sánchez et al., 2020; Mellone et al., 2015; Monje et al., 2020; Pifl et al., 2013, 2014). In this study, we

Table 1
PET scans performed for each radiotracer (^{18}F-FDG and ^{11}C-DTBZ), MPTP injections, and Kurlan scores across cases.

Group	^{18}F-FDG scans	^{11}C-DTBZ scans	MPTP injections[a]	Kurlan scores[a]	Description
Baseline	21	16	0 ± 0	0 ± 0	Monkeys before receiving MPTP.
Asymptomatic (n = 5)	5	4	2 ± 0	0 ± 0	No motor signs detected after the first two injections of MPTP.
Recovered (n = 6)	6	6	2.5 ± 0.9	0 ± 0	Spontaneous motor recovery after developing mild parkinsonian features for about 2–6 weeks.
Mild (n = 7)	7	6	4.1 ± 0.8	9.5 ± 3.8	Persistent, clearly recognizable but not intense parkinsonian features following 2–5 MPTP doses.
Severe (n = 19)	19	18	10.7 ± 2.5	19.7 ± 1.7	Severe and stable parkinsonism that exhibited prominent motor features.

[a] Data shown as mean ± SD.

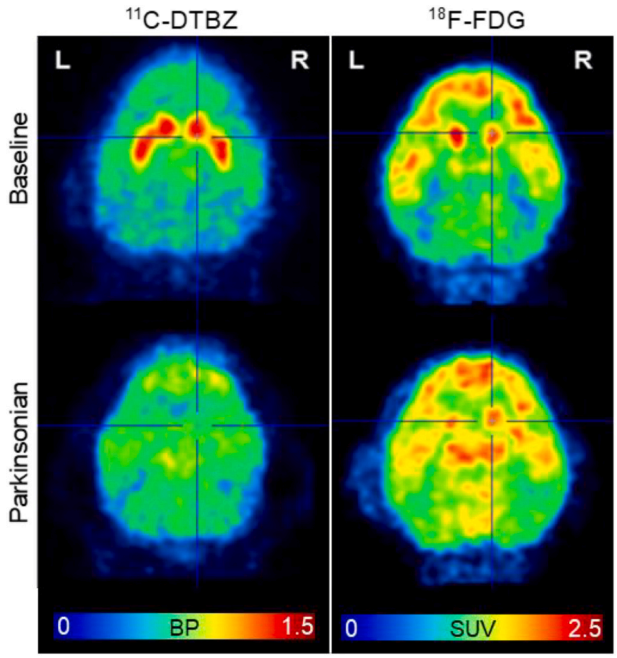

Fig. 1. Representative ^{11}C-DTBZ (left column) and ^{18}F-FDG (right column) PET images of one monkey at *control* (top row) and *severe* parkinsonian (bottom row) states. R: right; L: left.

estimated neuron population in a representative area (Brodmann's area 7) of the parietal cortex in four *control* and four *severe* parkinsonian monkeys to assess potential cortical neuron loss that could mediate cortical hypometabolism in parkinsonian monkeys. This region is also the most sensitive cortical area showing early cortical hypometabolism in PD patients.

2.3. PET scanning

PET imaging was performed in a dedicated small animal Philips MOSAIC tomograph (Cleveland, OH, USA). Animals were anesthetized by ketamine (10 mg/kg; i.m.) and midazolam (1 mg/kg; i.m.) and maintained during PET scanning with half of the initial dose per hour. Radiotracers were injected through the saphenous vein (bolus injection: 75 ± 10 MBq in 1 ml for ^{18}F-FDG and 72 ± 12 MBq in 1 ml for ^{11}C-DTBZ) (Quincoces et al., 2008). Care was taken to use the same dose of anesthesia for each monkey when repeating PET studies.

^{11}C-DTBZ PET studies were conducted as previously described (Collantes et al., 2008, 2009). Animals fasted overnight and baseline glucose was measured (51.8 ± 9.4 mg/dl) by taking a small drop of blood and subsequent reading in a glucose meter before ^{18}F-FDG injections. After each ^{18}F-FDG administration and 40 min of incorporation we performed static acquisition (20 min). All PET images were reconstructed as previously described (Collantes et al., 2008, 2009) (Fig. 1).

2.4. PET imaging analysis

Imaging data of radiotracers were processed using PMOD software (version 3.2; PMOD Technologies Ltd., Adliswil, Switzerland). ^{11}C-DTBZ PET images were spatially normalized into standard stereotaxic space using a species-specific template (Collantes et al., 2009). To develop a new ^{18}F-FDG PET template that served as reference in spatial normalization procedures of PET data, Brain Magnetic Resonance Imaging (MRI) of 15 *control* monkeys was undertaken on a 1.5 T Siemens Symphony scanner (Erlangen, Germany) (Fig. 2), as previously described (Collantes et al., 2009). ^{11}C-DTBZ PET studies were transformed by calculating binding potential (BP) of vesicular monoamine transporter 2 and obtaining parametric images as described previously (Collantes et al., 2009; Ichise et al., 2001). ^{18}F-FDG PET images were transformed into semi-quantitative images representing standardized uptake value (SUV), using the injected radiotracer dose and animal body weight. Then, all ^{18}F-FDG images were masked to remove extra-cerebral signals that would disrupt the global normalization, and a Gaussian-smoothing kernel of 4 mm was applied.

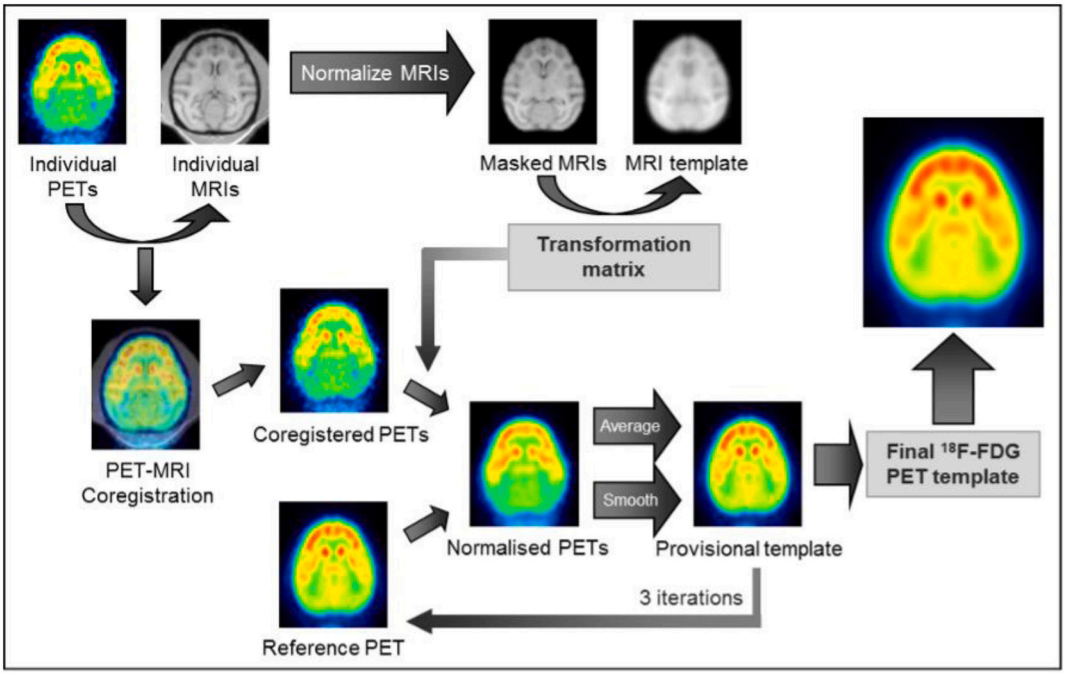

Fig. 2. Stepwise process to obtain from baseline ^{18}F-FDG PET and MRI images (top left) the final ^{18}F-FDG PET template of the monkey brain (far right).

2.5. Image analysis

^{11}C-DTBZ images were studied using a volume of interest (VOI) analysis. A VOI template map including the striatum was applied over the images to extract the average BP striatal values. Differences in ^{18}F-FDG SUV values between groups were assessed using voxel-based SPM8 software (Wellcome Department of Cognitive Neurology, Institute of Neurology, London, UK). As each animal could be imaged at different states, one-way ANOVA within subjects was performed, using blood glucose measurements as covariate. Model parameters included global normalization with ANCOVA (by including the global covariate in the general linear model) and relative threshold masking at 80% of mean voxel value. Comparisons were made for decreases and increases in ^{18}F-FDG uptake allowing voxels of significant relative change between groups to be identified throughout the whole brain. Significant parametric maps were rendered over a spatially normalized MRI image and were anatomically evaluated and located using a VOI map for the identification of brain regions.

Voxel-based regression analysis was conducted to assess the relationship between metabolism and dopaminergic deficit by using the following covariates: striatal ^{11}C-DTBZ BP values, Kurlan score and glucose measurements. SPM based correlation analysis was performed with data from animals scanned with both radiotracers at different motor states (Table 1).

2.6. Unbiased stereology of neuron population and volume analysis in the cortex

We estimated the entire neuron population in a representative area (Brodmann's area 7) of the parietal cortex in Nissl-stained sections of *control* and *severe* parkinsonian monkeys [for tissue processing see (Blesa et al., 2012)]. Nissl technique colors the nuclei and bodies of all neurons in the stained tissue, allowing for estimation of entire neuron populations (García-Cabezas et al., 2016). Nissl technique also provides cytoarchitectonic pictures of the cerebral cortex allowing for area identification (García-Cabezas and Barbas, 2014).

First, we examined the parietal cortex in coronal sections of the brain stained with Nissl under low magnification optical microscopy to identify the boundaries of Brodmann's area 7. This area lies between the intraparietal sulcus and the end of the superior temporal sulcus (Cavada and Goldman-Rakic, 1989).We selected eight serial Nissl-stained coronal sections (one every tenth; 40 μm thick) in four *control* and four *severe* parkinsonian monkeys and delineated the boundaries of Brodmann's area 7 on each selected section under 2× magnification objective with the aid of a semiautomated commercial system (StereoInvestigator; MicroBrightField, Williston, VT, USA). We sampled systematically the entire volume of Brodmann's area 7 in each case through the selected sections to count neurons that were identified using 100× oil-immersion according to cytological features (García-Cabezas et al., 2016). The top and bottom of each section (minimum 2 μm for 8 μm sections after shrinkage) were used as guard zones and the actual mounted section thickness was measured at each counting site. The counting frame/dissector size (60 × 60 μm, height = 8 μm) and grid spacing (2000 × 2000 μm) were set to yield a coefficient of error for neuron population below 0.10 (Gundersen, m = 0) and 0.05 (Gundersen, m = 1), as recommended (Howard and Reed, 1998). Cavalieri's principle was used to estimate the volume of Brodmann's area 7 across cases. Neuron density was obtained by dividing the estimated neuron population in Brodmann's area 7 by the estimated volume of this area in each case.

2.7. Statistics

Average striatal BP values were tested for normality (Skewness/Kurtosis tests) and homogeneity of variances (Levene's test). When normality could be assumed, differences in BP values between *control* and MPTP treated groups were assessed using unpaired two-sample *t*-test followed by False Discovery Rate correction for multiple comparisons. The significance level was set at a corrected *P*-value <0.05. All statistical analysis and data management was performed using R version 1.1.463.

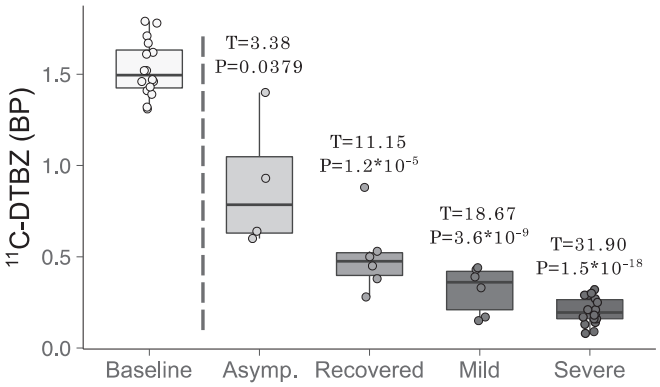

Fig. 3. Boxplots of striatal ^{11}C-DTBZ binding potential (BP) in *baseline (n = 16), asymptomatic (n = 4), recovered (n = 6), mild (n = 6),* and *severe* MPTP treated monkeys (*n* = 18). Statistical comparison of ^{11}C-DTBZ BP differences between MPTP treated (*asymptomatic, recovered, mild* and *severe*) and *control* groups was performed using an unpaired two-sample t-test. T-scores and *P*-values (after false discovery rate correction for multiple comparisons) are included above each box.

In the voxel-based analyses, significance level threshold was set at an uncorrected P-value <0.001. To show some clusters of hypometabolism representing in the following groups in the *asymptomatic* group, we relaxed our significance cut-off to P-value <0.01 in the comparison between *asymptomatic* and *control* groups. Statistical significance in the voxel-based regression analysis was set at P-value <0.05 after family-wise error (FEW) correction for multiple comparisons at the voxel level.

3. Results

3.1. Cerebral metabolic patterns and progressive striatal dopamine depletion

Striatal ^{11}C-DTBZ BP values decreased with increasing motor impairment and higher MPTP dosing across groups (Fig. 3), as described before (Blesa et al., 2010, 2012).

Metabolic patterns evolved in parallel with progressive striatal dopamine depletion; early cortical hypometabolism in temporal and parietal cortices was present in *asymptomatic* monkeys (∼40% dopaminergic striatal deficit) and spread to adjacent areas from initial foci in *recovered, mild,* and *severe* monkeys. In *severe* parkinsonian monkeys, hypometabolism persisted in temporal and parietal areas and extended to lateral-frontal cortices (Fig. 4A-B).

Hypermetabolism emerged in globus pallidus (GP) pars interna and cerebellum in *mild* parkinsonian monkeys, spreading to adjacent areas in these regions and extending to the thalamus and mid-brainstem in *severe* parkinsonian monkeys. Hypermetabolism was not observed in *asymptomatic* and *recovered* monkeys in keeping with normal motor status (Fig. 4C).

3.2. Correlation of motor behavior, striatal dopaminergic depletion, and cerebral metabolism

Correlation analysis revealed positive relationship between striatal dopamine depletion (measured by ^{11}C-DTBZ PET) and hypometabolism in posterior temporal, parietal, and lateral-frontal cortices (measured by ^{18}F-FDG PET). Also, there was negative relationship between dopamine depletion and GP and thalamus hypermetabolism (Fig. 5A-B). Motor behavior (measured by Kurlan score) correlated negatively with

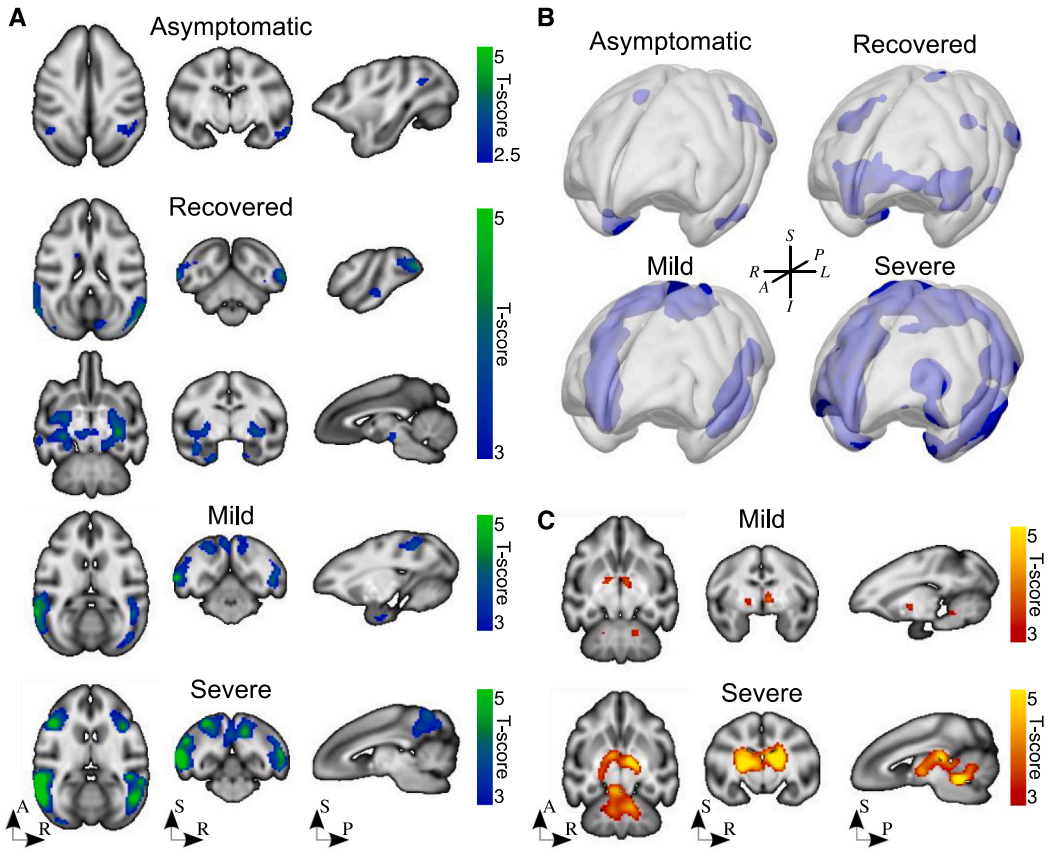

Fig. 4. Cerebral metabolic patterns across motor stages (*asymptomatic, recovered, mild,* and *severe)* of progressively MPTP treated monkeys. (A) Statistical T-map of SPM PET analysis over spatially normalized MRI shows progressive spreading of hypometabolism (lower ^{18}F-FDG uptake than *control* group) across cortical regions. (B) Rendering of hypometabolic patterns of fig. (A) in 3D glass brains. (C) Statistical T-map of SPM PET analysis over spatially normalized MRI shows hypermetabolism (higher ^{18}F-FDG uptake than *control* group) in subcortical regions for *mild* and *severe* parkinsonian monkeys. *Asymptomatic* and *recovered* groups did not show hypermetabolism. SPM results were obtained by ANOVA within monkeys at different motor states compared with *control* monkeys ($P < 0.001$ uncorrected). A: anterior; P: posterior; R: right; L: left; S: superior; I: inferior. Sample sizes for the different groups used in this analysis were: *control* ($n = 21$), *asymptomatic* ($n = 5$), *recovered* ($n = 6$), *mild* ($n = 7$), and *severe* parkinsonian ($n = 19$).

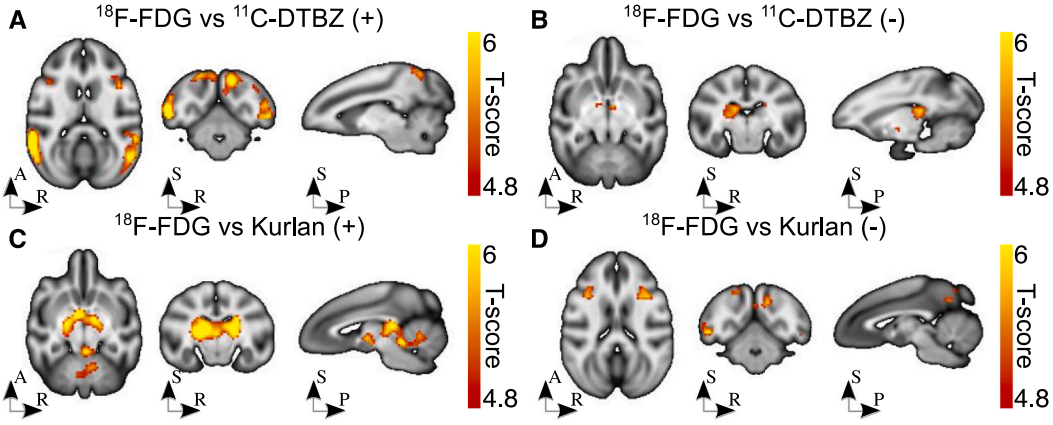

Fig. 5. T-maps over spatially normalized MRI image showing significant correlations of cerebral metabolic changes with striatal dopamine depletion and motor state. Positive (A) and negative (B) correlation between cerebral metabolic changes (^{18}F-FDG uptake) and striatal dopaminergic depletion (^{11}C-DTBZ BP values). Positive (C) and negative (D) correlation between cerebral metabolic changes (^{18}F-FDG uptake) and motor state (Kurlan scores). Significance threshold of $P < 0.05$ (FWE corrected at the voxel level) was applied. Color bars represent T-score. A: anterior; P: posterior; R: right; L: left; S: superior; I: inferior.

hypometabolism in the lateral-frontal cortex, and positively with hypermetabolism in GP, thalamus, and cerebellum (Fig. 5C-D). These results provide firm evidence for strong relationship between motor behavior, striatal dopaminergic depletion, and cerebral metabolic changes in parkinsonism. No correlations were found between ^{18}F-FDG uptake and blood glucose measurement.

3.3. Neuron population and neuron density in the parietal cortex

Brodmann's area 7 in the parietal cortex showed normal laminar structure, normal neuron distribution, and normal neuron body size in Nissl-stained sections of *control* and *severe* parkinsonian monkeys (Fig. 6). In *control* cases, the entire neuron population in Brodmann's area 7 ranged between 8,887,651 and 13,377,225 neurons (mean = 11,847,083 ± 2,028,822 neurons) and neuron density ranged between 55,154 and 85,805 neurons/mm^3 (mean = 71,918 ± 12,734 neurons/mm^3). These estimates of neuron density in Brodmann's area 7 obtained in *control* monkeys were comparable to estimates of Brodmann's area 7 obtained in previous studies with unbiased stereological methods (Medalla and Barbas, 2006). In *severe* monkeys, the entire neuron population in Brodmann's area 7 ranged between 10,123,896 and 15,606,120 neurons/mm^3 (mean = 13,395,839 ± 2,321,569 neurons) and neuron density ranged between 63,192 and 95,183 neurons/mm^3 (mean = 80,665 ± 14,806 neurons/mm^3). ANOVA didn't show statistically significant differences in neuron population, area volume, and neuron density of Brodmann's area 7 between *control* and *severe* monkeys (Fig. 6C-D-E).

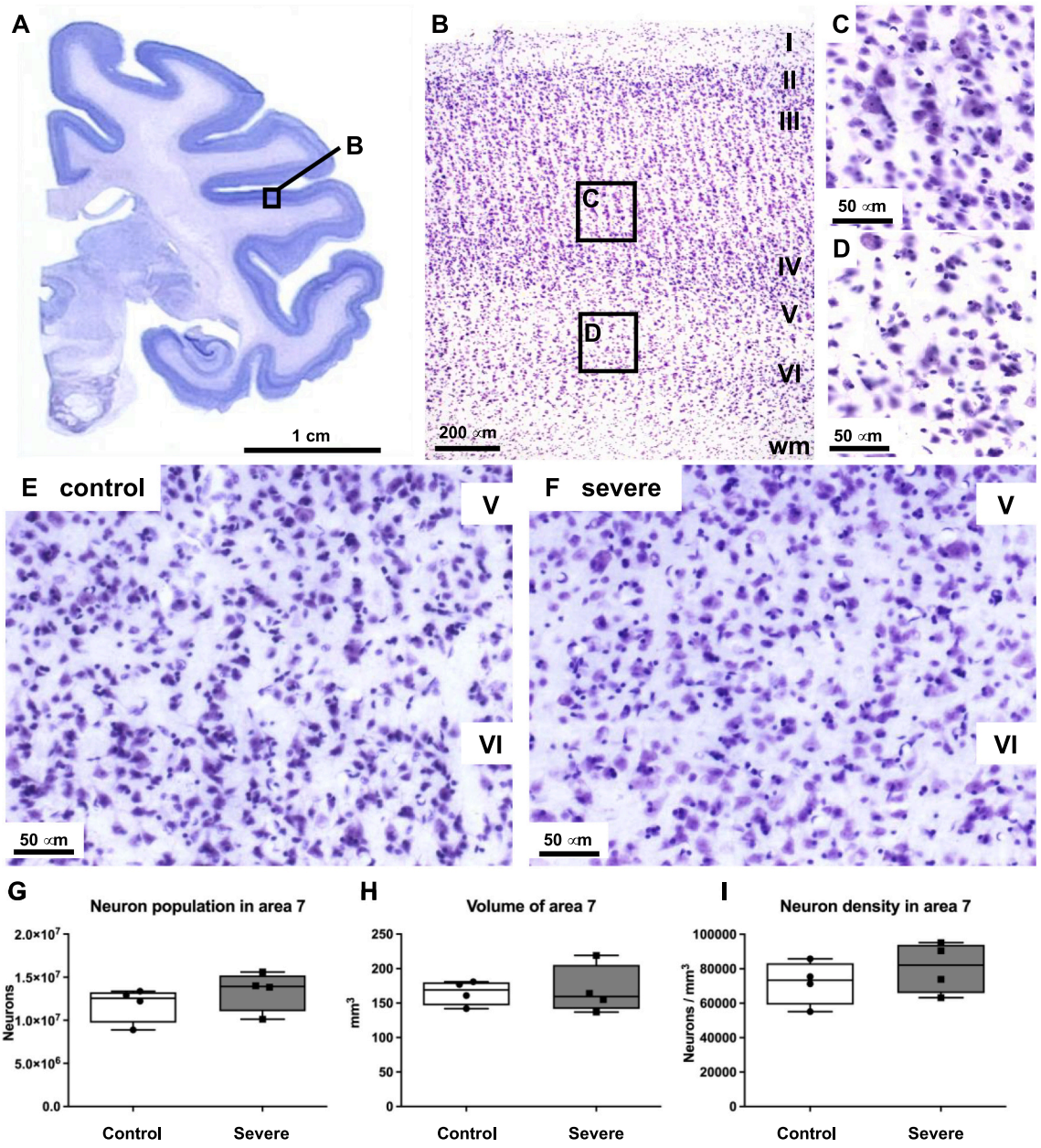

Fig. 6. Microscopic structure of Brodmann's area 7 in the parietal cortex. (A) Nissl-stained coronal section through Brodmann's area 7 in a *control* monkey. (B) Magnified micrograph of Brodmann's area 7. (C-D) Magnified micrographs of superficial and deep layers in Brodmann's area 7. Micrographs of Brodmann's area 7 in *control* (E) and *severe* parkinsonian monkeys (F). Bar-plots comparing neuron population (G), total volume (H), and neuron density of area 7 (I) between *control* and *severe* parkinsonian monkeys (n = 4/group). Roman numerals indicate cortical layers; wm: white matter.

4. Discussion

In this paper we show that changes in cerebral metabolism are associated with progressive depletion of striatal dopamine in the MPTP monkey model. This model allows us to distinguish progressive states of dopaminergic loss that mimic the evolution of parkinsonism in PD patients. The main finding in this paper is the emergence of early cortical hypometabolism in parallel with modest nigrostriatal dopaminergic depletion. Remarkably, the cerebral metabolic pattern found here can be paralleled overall with the Parkinson's disease Related Pattern (PDRP), which is a motor-related spatial covariance PET pattern described in PD patients (Eidelberg, 2009; Ma et al., 2007; Spetsieris and Eidelberg, 2011). Most significant features of the PDRP are recapitulated in the progressive MPTP monkey model, including hypermetabolism in GP, thalamus, cerebellum, and pons, as well as hypometabolism in lateral-frontal (premotor) and parieto-temporal cortices; cortical hypometabolism in parieto-temporal cortices and subcortical hypermetabolism in GP, cerebellum, and thalamus have been reported in other studies in stable parkinsonian monkeys (Emborg et al., 2007; Guigoni et al., 2005; Ma et al., 2012, 2015; Mitchell et al., 1989).

4.1. Pre-symptomatic changes: cortical hypometabolism

Studying pre-symptomatic stages of PD in humans is extremely difficult and impractical due to difficulties of diagnosis and low number of subjects with genetic PD available. To the best of our knowledge, this is the first report of cerebral metabolic changes in pre-symptomatic MPTP-monkeys. Our results are coherent with prior reports on functional abnormalities in *de novo* drug-naïve and early-stage PD patients (Arnaldi et al., 2016; Huang et al., 2007; Sala et al., 2017; Schindlbeck et al., 2019; Tang et al., 2011; Zeighami et al., 2015).

The metabolic changes observed in non-treated PD patients are likely to have developed several years prior to the onset of clinical signs and include hypometabolism in cortical regions included in the PDRP (Schindlbeck et al., 2019). The origin and significance of reduction/increment in FDG-PET in PD and in MPTP-treated monkeys is not straightforward. We consider that hypometabolism can essentially be explained because of 1. Cellular loss or reduced microglia activity/changes in the affected regions (Xiang et al., 2021); 2. Reduced metabolic/energy demand. This in turn may be because of *i)* Reduced excitatory input; *ii)* Increased inhibitory activity. Thus, both local neuronal and microglia activity could contribute to the FDG signal with their relative contribution probably depending on how advanced the pathology for any given region.

Cortical pathology is a well-recognized feature of PD but is not associated with changes very early in the evolution (Blesa et al., 2021). Changes in microglial activity has been recently suggested to be a principal factor modulating glucose consumption (Xiang et al., 2021). Regarding functional changes, cortical studies (with magnetic cortical stimulation) of the motor cortex in PD patients has shown that cortical disinhibition is a very early, possibly prodromal feature of PD making enhanced intra-cortical inhibition an improbable mechanism of hypometabolism (Ammann et al., 2020). On the other hand, afferent cortical aminergic deafferentation has been recently shown in parkinsonian monkeys (Masilamoni et al., 2021) and data from PD patients suggest that cortical hypometabolism probably arises in relation with nigrostriatal impairment (Orso et al., 2021; Ruppert et al., 2020). More specifically, temporo-parietal hypometabolism correlated with caudate dopaminergic depletion in PD patients whereas pre-frontal hypometabolism correlates with serotoninergic deafferentation in the thalamus (Orso et al., 2021). Certainly, dopaminergic denervation of the dorsal caudate and thalamus is an early feature of the MPTP monkey model (Blesa et al., 2012; Monje et al., 2020; Villalba et al., 2009). The reduction in glucose uptake becomes more severe and widespread across cortical areas along with progression of striatal dopaminergic depletion and greater cortical aminergic loss both in PD patients and MPTP monkeys (Masilamoni et al., 2021; Pifl et al., 1992). Altogether, the available data allow us to suggest that reduced afferent driving could be a relevant mechanism explaining the findings here discussed.

Certainly, our study was not planned at the time with a net expectation of finding cortical hypometabolism. However, radiotracer to assess noradrenaline, serotonin and acetylcholine cortical innervation are now being developed and actually applied to PD (Strafella et al., 2017). This may be further optimized by refined MRI methodology which encounters cortical thickness reduction in *de novo* PD patients (Laansma et al., 2021). Conceivably, it will soon be possible to undertake such studies and correlate with cortical hypometabolism in early PD patients and asymptomatic MPTP monkeys.

4.2. Methodological validity and reproducibility

The major limitation of this study is that cortical hypometabolism was not necessarily conceived as a primary, fundamental finding of the study and, we had not anticipated so early changes in the parieto-temporal region. This would have necessitated a specific design to test monkeys' behavior and evaluate in some detail cognitive performance. The motor assessment routinely used in our laboratory cannot possibly detect potential alterations of visuo-spatial functioning typically sustained by the parieto-temporal cortex. Thus, we cannot establish any specific significance to the cortical hypometabolism described here. Nevertheless, we believe the findings are very relevant because provide strong support to the clinical FDG-PET findings in early PD patients and opens the possibility of further defining the underlying mechanisms. This, in turn, could be relevant when therapeutic options to modify PD evolution become finally available.

Admittedly, a relevant point for the initial changes in the asymptomatic stage concerns that cortical changes are somewhat asymmetrical at the parietal cortex, whereas in the other groups, with greater dopamine depletion, the changes are more bilaterally distributed. We believe that the averaged template of FDG-PET uptake can hardly be expected to be totally symmetrical because of individual variations and even the nigrostriatal lesion is not entirely identical and symmetrical, certainly less in the asymptomatic stage where the denervation is less prominent.

Thus, despite the well-known individual variations among monkeys, cerebral metabolic changes of progressive MPTP treated monkeys were relatively homogenous for each stage. Indeed, the cerebral metabolic patterns found here in stable parkinsonian monkeys closely reproduce brain metabolic changes described in previous studies (Ma et al., 2012, 2015), in spite of using different monkey species, different MPTP administration regimen, and some other methodological differences, further supporting reproducibility and validity of our data.

5. Conclusions

We show that early striatal dopaminergic depletion in the progressive MPTP monkey model of PD is associated with cortical hypometabolism in cortical areas and hypermetabolism in GP, thalamus, and cerebellum, mimicking by and large the metabolic pattern described in PD. Reduction of temporo-parietal cortical metabolism appear early in the evolution of dopaminergic depletion in the asymptomatic stage and are not related to neuronal loss in the cortex. The study of early cerebral metabolic changes in pre-symptomatic MPTP lesioned monkeys are likely to provide valid information concerning the effects of putative therapies aiming to modify disease evolution.

Author statement

FMD, MC, EI, EP and ME performed the imaging PET studies. FMD, JB, CJ, JPP, RRR, EP and MCR analyzed the data from the imaging studies.

MC, EP and IP supervised the imaging PET studies and analyzed the

data.

JB, ITD, EI, LFH and BG performed the behavior studies with the animals and analyzed the data.

JB, NLG, MGC and CC performed the histological experiments and analyzed the data.

MCR, IP and JAO designed the study.

FMD, JB and JAO wrote the manuscript.

All the authors contributed to discussion of content, reviewing or editing the manuscript.

Declaration of Competing Interest

The authors declare that there are no conflicts of interest.

Acknowledgments

We thank the cyclotron staff of the Nuclear Medicine Department and PET-GMP Laboratory of Clínica Universidad de Navarra for radiotracer production. This research was supported by UTE-CIMA agreement of the University of Navarra, Grant S2017/BMD-3700 (NEUROMETAB-CM) from Comunidad de Madrid and co-financed with the Structural Funds of the European Union; Fundación Jesús de Gangoiti (Bilbao, Spain); Miguel Servet contract form ISCIII (CP15/00200) to J.B; Beatriz Galindo senior research position in the Faculty of Medicine (BEAGAL18/00098) and a Grant for I + D Projects for the Beatriz Galindo Program Researchers at Universidad Autónoma de Madrid (SI2/PBG/2020-00014) to M.A.G-C; Chair in Neuroscience UAM-Fundación Tatiana Pérez de Guzmán el Bueno to C.C.

References

Ammann, C., Dileone, M., Pagge, C., Catanzaro, V., Mata-Marín, D., Hernández-Fernández, F., Monje, M.H.G.G., Sánchez-Ferro, Á., Fernández-Rodríguez, B., Gasca-Salas, C., Máñez-Miró, J.U., Martínez-Fernández, R., Vela-Desojo, L., Alonso-Frech, F., Oliviero, A., Obeso, J.A., Foffani, G., 2020. Cortical disinhibition in Parkinson's disease. Brain 143, 3408–3421. https://doi.org/10.1093/brain/awaa274.

Arnaldi, D., Morbelli, S., Brugnolo, A., Girtler, N., Picco, A., Ferrara, M., Accardo, J., Buschiazzo, A., de Carli, F., Pagani, M., Nobili, F., 2016. Functional neuroimaging and clinical features of drug naive patients with de novo Parkinson's disease and probable RBD. Parkinsonism Relat. Disord. 29, 47–53. https://doi.org/10.1016/j.parkreldis.2016.05.031.

Blesa, J., Juri, C., Collantes, M., Peñuelas, I., Prieto, E., Iglesias, E., Martí-Climent, J., Arbizu, J., Zubieta, J.L., Rodríguez-Oroz, M.C., García-García, D., Richter, J.A., Cavada, C., Obeso, J.A., 2010. Progression of dopaminergic depletion in a model of MPTP-induced Parkinsonism in non-human primates. An 18F-DOPA and 11C-DTBZ PET study. Neurobiol. Dis. 38, 456–463. https://doi.org/10.1016/j.nbd.2010.03.006.

Blesa, J., Juri, C., García-Cabezas, M.Á., Adánez, R., Sánchez-González, M.Á., Cavada, C., Obeso, J.A., 2011. Inter-hemispheric asymmetry of nigrostriatal dopaminergic lesion: a possible compensatory mechanism in Parkinson's disease. Front. Syst. Neurosci. 5, 92. https://doi.org/10.3389/fnsys.2011.00092.

Blesa, J., Pifl, C., Sánchez-González, M.A., Juri, C., García-Cabezas, M., Adánez, R., Iglesias, E., Collantes, M., Peñuelas, I., Sánchez-Hernández, J.J., Rodríguez-Oroz, M. C., Avendaño, C., Hornykiewicz, O., Cavada, C., Obeso, J.A., 2012. The nigrostriatal system in the presymptomatic and symptomatic stages in the MPTP monkey model : a PET , histological and biochemical study. Neurobiol. Dis. 48, 79–91. https://doi.org/10.1016/j.nbd.2012.05.018.

Blesa, J., Trigo-Damas, I., Dileone, M., Lopez-Gonzalez del Rey, N., Hernandez, L.F., Obeso, J.A., 2017. Compensatory mechanisms in Parkinson's disease: circuits adaptations and role in disease modification. Exp. Neurol. 298, 148–161. https://doi.org/10.1016/j.expneurol.2017.10.002.

Blesa, J., Foffani, G., Dehay, B., Bezard, E., Obeso, J.A., 2021. Motor and non-motor circuit disturbances in early Parkinson disease: which happens first? Nat. Rev. Neurosci. https://doi.org/10.1038/S41583-021-00542-9.

Cavada, C., Goldman-Rakic, P.S., 1989. Posterior parietal cortex in rhesus monkey: I. Parcellation of areas based on distinctive limbic and sensory corticocortical connections. J. Comp. Neurol. 287, 393–421. https://doi.org/10.1002/CNE.902870402.

Collantes, M., Peñuelas, I., Alvarez-Erviti, L., Blesa, J., Martí-Climent, J.M., Quincoces, G., Delgado, M., Ecay, M., Martínez, A., Arbizu, J., Rodríguez-Oroz, M.C., Obeso, J., Richter, J.A., 2008. Use of 11C-(+)-alpha -dihydrotetrabenazine for the assessment of dopaminergic innervation in animal models of Parkinson's disease. Rev. española Med. Nucl. 27, 103–111.

Collantes, M., Prieto, E., Peñuelas, I., Blesa, J., Juri, C., Martí-Climent, J.M., Quincoces, G., Arbizu, J., Riverol, M., Zubieta, J.L., Rodriguez-Oroz, M.C., Luquin, M.R., Richter, J.A., Obeso, J.A., 2009. New MRI, 18F-DOPA and 11C-(+)-alpha-dihydrotetrabenazine templates for Macaca fascicularis neuroimaging: advantages to improve PET quantification. Neuroimage 47, 533–539. https://doi.org/10.1016/j.neuroimage.2009.04.078.

de la Fuente-Fernandez, R., Schulzer, M., Kuramoto, L., Cragg, J., Ramachandiran, N., Au, W.L., Mak, E., McKenzie, J., McCormick, S., Sossi, V., Ruth, T.J., Lee, C.S., Calne, D.B., Stoessl, A.J., 2011. Age-specific progression of nigrostriatal dysfunction in Parkinson's disease. Ann. Neurol. 69, 803–810.

Del Rey, N.L.-G.L.-G., Quiroga-Varela, A., Garbayo, E., Carballo-Carbajal, I., Fernández-Santiago, R., Monje, M.H.G., Trigo-Damas, I., Blanco-Prieto, M.J., Blesa, J., 2018. Advances in Parkinson's disease: 200 years later. Front. Neuroanat. 12, 113. https://doi.org/10.3389/fnana.2018.00113.

Eckert, T., Barnes, A., Dhawan, V., Frucht, S., Gordon, M.F., Feigin, A.S., Eidelberg, D., 2005. FDG PET in the differential diagnosis of parkinsonian disorders. Neuroimage 26, 912–921. https://doi.org/10.1016/j.neuroimage.2005.03.012.

Eckert, T., Tang, C., Eidelberg, D., 2007. Assessment of the progression of Parkinson's disease: a metabolic network approach. Lancet Neurol. 6, 926–932.

Eidelberg, D., 2009. Metabolic brain networks in neurodegenerative disorders: a functional imaging approach. Trends Neurosci. 32, 548–557. https://doi.org/10.1016/j.tins.2009.06.003.

Emborg, M.E., Carbon, M., Holden, J.E., During, M.J., Ma, Y., Tang, C., Moirano, J., Fitzsimons, H., Roitberg, B.Z., Tuccar, E., Roberts, A., Kaplitt, M.G., Eidelberg, D., 2007. Subthalamic glutamic acid decarboxylase gene therapy: changes in motor function and cortical metabolism. J. Cereb. Blood Flow Metab. 27, 501–509. https://doi.org/10.1038/sj.jcbfm.9600364.

Enterría-Morales, D., del Rey, N.L.-G., Blesa, J., López-López, I., Gallet, S., Prévot, V., López-Barneo, J., d'Anglemont de Tassigny, X., 2020. Molecular targets for endogenous glial cell line-derived neurotrophic factor modulation in striatal parvalbumin interneurons. Brain Commun. 2 https://doi.org/10.1093/braincomms/fcaa105.

García-Cabezas, M.Á., Barbas, H., 2014. Area 4 Has Layer IV in Adult Primates, 39, pp. 1824–1834. https://doi.org/10.1111/EJN.12585.

García-Cabezas, M.Á., John, Y.J., Barbas, H., Zikopoulos, B., 2016. Distinction of neurons, glia and endothelial cells in the cerebral cortex: an algorithm based on cytological features. Front. Neuroanat. 0, 107. https://doi.org/10.3389/FNANA.2016.00107.

Guigoni, C., Li, Q., Aubert, I., Dovero, S., Bioulac, B.H., Bloch, B., Crossman, A.R., Gross, C.E., Bezard, E., 2005. Involvement of sensorimotor, limbic, and associative basal ganglia domains in L-3,4-dihydroxyphenylalanine-induced dyskinesia. J. Neurosci. 25, 2102–2107. https://doi.org/10.1523/JNEUROSCI.5059-04.2005.

Hirano, S., Eckert, T., Flanagan, T., Eidelberg, D., 2009. Metabolic networks for assessment of therapy and diagnosis in Parkinson's disease. Mov. Disord. 24 (Suppl. 2), S725–S731. https://doi.org/10.1002/mds.22541.

Howard, C.V., Reed, M.G., 1998. Unbiased Stereology. BIOS Scientific Publishers Limited.

Huang, C., Tang, C., Feigin, A., Lesser, M., Ma, Y., Pourfar, M., Dhawan, V., Eidelberg, D., 2007. Changes in network activity with the progression of Parkinson's disease. Brain 130, 1834–1846 [pii]. https://doi.org/10.1093/brain/awm086.

Ichise, M., Meyer, J.H., Yonekura, Y., 2001. An introduction to PET and SPECT neuroreceptor quantification models. J. Nucl. Med. 42, 755–763.

Jiménez-Sánchez, L., Blesa, J., Del Rey, N.L., Monje, M.H.G., Obeso, J.A., Cavada, C., 2020. Serotonergic innervation of the striatum in a nonhuman primate model of Parkinson's disease. Neuropharmacology 170. https://doi.org/10.1016/j.neuropharm.2019.107806.

Laansma, M.A., Bright, J.K., Al-Bachari, S., Anderson, T.J., Ard, T., Assogna, F., Baquero, K.A., Berendse, H.W., Blair, J., Cendes, F., Dalrymple-Alford, J.C., de Bie, R.M.A., Debove, I., Dirkx, M.F., Druzgal, J., Emsley, H.C.A., Garraux, G., Guimarães, R.P., Gutman, B.A., Helmich, R.C., Klein, J.C., Mackay, C.E., McMillan, C.T., Melzer, T.R., Parkes, L.M., Piras, F., Pitcher, T.L., Poston, K.L., Rango, M., Ribeiro, L.F., Rocha, C.S., Rummel, C., Santos, L.S.R., Schmidt, R., Schwingenschuh, P., Spalletta, G., Squarcina, L., van den Heuvel, O.A., Vriend, C., Wang, J.-J., Weintraub, D., Wiest, R., Yasuda, C.L., Jahanshad, N., Thompson, P.M., van der Werf, Y.D., 2021. International multicenter analysis of brain structure across clinical stages of Parkinson's disease. Mov. Disord. https://doi.org/10.1002/MDS.28706.

Ma, Y., Tang, C., Spetsieris, P.G., Dhawan, V., Eidelberg, D., 2007. Abnormal metabolic network activity in Parkinson'S disease: test—retest reproducibility. J. Cereb. Blood Flow Metab. 27, 597–605. https://doi.org/10.1038/sj.jcbfm.9600358.

Ma, Y., Peng, S., Spetsieris, P.G., Sossi, V., Eidelberg, D., Doudet, D.J., 2012. No Title, p. 32. https://doi.org/10.1038/jcbfm.2011.166.

Ma, Y., Johnston, T.H., Peng, S., Zuo, C., Koprich, J.B., Fox, S.H., Guan, Y., Eidelberg, D., Brotchie, J.M., 2015. Reproducibility of a Parkinsonism-related metabolic brain network in non-human primates: a descriptive pilot study with FDG PET. Mov. Disord. 30, 1283–1288. https://doi.org/10.1002/mds.26302.

Masilamoni, G.J., Weinkle, A., Papa, S.M., Smith, Y., 2021. Cortical serotonergic and catecholaminergic denervation in MPTP-treated parkinsonian monkeys. Cereb. Cortex. https://doi.org/10.1093/CERCOR/BHAB313.

Medalla, M., Barbas, H., 2006. Diversity of laminar connections linking periarcuate and lateral intraparietal areas depends on cortical structure. Eur. J. Neurosci. 23, 161–179. https://doi.org/10.1111/J.1460-9568.2005.04522.X.

Meles, S.K., Renken, R.J., Pagani, M., Teune, L.K., Arnaldi, D., Morbelli, S., Nobili, F., van Laar, T., Obeso, J.A., Rodríguez-Oroz, M.C., Leenders, K.L., 2019. Abnormal pattern of brain glucose metabolism in Parkinson's disease: replication in three European cohorts. Eur. J. Nucl. Med. Mol. Imaging 47, 437–450. https://doi.org/10.1007/S00259-019-04570-7, 2019 472.

Mellone, M., Stanic, J., Hernandez, L.F., Iglesias, E., Zianni, E., Longhi, A., Prigent, A., Picconi, B., Calabresi, P., Hirsch, E.C., Obeso, J.A., Di Luca, M., Gardoni, F., 2015.

NMDA receptor GluN2A/GluN2B subunit ratio as synaptic trait of levodopa-induced dyskinesias: from experimental models to patients. Front. Cell. Neurosci. 9, 245. https://doi.org/10.3389/fncel.2015.00245.

Mitchell, I.J., Clarke, C.E., Boyce, S., Robertson, R.G., Peggs, D., Sambrook, M.A., Crossman, A.R., 1989. Neural mechanisms underlying parkinsonian symptoms based upon regional uptake of 2-deoxyglucose in monkeys exposed to 1-methyl-4-phenyl-1,2,3,6-tetrahydropyridine. Neuroscience 32, 213–226.

Monje, M.H.G., Blesa, J., García-Cabezas, M.Á., Obeso, J.A., Cavada, C., 2020. Changes in thalamic dopamine innervation in a progressive Parkinson's disease model in monkeys. Mov. Disord. 35, 419–430. https://doi.org/10.1002/mds.27921.

Nandhagopal, R., Kuramoto, L., Schulzer, M., Mak, E., Cragg, J., McKenzie, J., McCormick, S., Ruth, T.J., Sossi, V., de la Fuente-Fernandez, R., Stoessl, A.J., 2011. Longitudinal evolution of compensatory changes in striatal dopamine processing in Parkinson's disease. Brain 134, 3290–3298.

Niethammer, M., Feigin, A., Eidelberg, D., 2012. Functional neuroimaging in Parkinson's disease. Cold Spring Harb. Perspect. Med. 2 https://doi.org/10.1101/cshperspect.a009274.

Orso, B., Arnaldi, D., Girtler, N., Brugnolo, A., Doglione, E., Mattioli, P., Biassoni, E., Fancellu, R., Massa, F., Bauckneht, M., Chiola, S., Morbelli, S., Nobili, F., Pardini, M., 2021. Dopaminergic and Serotonergic Degeneration and Cortical [18F] Fluorodeoxyglucose Positron Emission Tomography in De Novo Parkinson's Disease. Mov. Disord.

Pifl, C., Schingnitz, G., Hornykiewicz, O., 1992. Striatal and non-striatal neurotransmitter changes in MPTP-parkinsonism in rhesus monkey: the symptomatic versus the asymptomatic condition. Neurochem. Int. 20 (Suppl), 295S–297S.

Pifl, C., Hornykiewicz, O., Blesa, J., Adánez, R., Cavada, C., Obeso, J.A., 2013. Reduced noradrenaline, but not dopamine and serotonin in motor thalamus of the MPTP primate: relation to severity of parkinsonism. J. Neurochem. 125, 657–662. https://doi.org/10.1111/jnc.12162.

Pifl, C., Rajput, A.H.A., Reither, H., Blesa, J., Cavada, C., Obeso, J.A., Rajput, A.H.A., Hornykiewicz, O., 2014. Is Parkinson's disease a vesicular dopamine storage disorder? Evidence from a study in isolated synaptic vesicles of human and nonhuman primate striatum. J. Neurosci. 34, 8210–8218. https://doi.org/10.1523/JNEUROSCI.5456-13.2014.

Pifl, C., Reither, H., del Rey, N.L.G., Cavada, C., Obeso, J.A., Blesa, J., 2017. Early paradoxical increase of dopamine: a neurochemical study of olfactory bulb in asymptomatic and symptomatic MPTP treated monkeys. Front. Neuroanat. 11 https://doi.org/10.3389/fnana.2017.00046.

Quincoces, G., Collantes, M., Catalán, R., Ecay, M., Prieto, E., Martino, E., Blesa, F.J., Alvarez-Erviti, L., Areses, P., Arbizu, J., Obeso, J.A., Martí-Climent, J.M., Richter, J. A., Peñuelas, I., 2008. Quick and simple synthesis of (11)C-(+)-alpha-dihydrotetrabenazine to be used as a PET radioligand of vesicular monoamine transporters. Rev. española Med. Nucl. 27, 13–21.

Ruppert, M.C., Greuel, A., Tahmasian, M., Schwartz, F., Stürmer, S., Maier, F., Hammes, J., Tittgemeyer, M., Timmermann, L., van Eimeren, T., Drzezga, A., Eggers, C., 2020. Network degeneration in Parkinson's disease: multimodal imaging of nigro-striato-cortical dysfunction. Brain 143, 944–959. https://doi.org/10.1093/brain/awaa019.

Sala, A., Caminiti, S.P., Presotto, L., Premi, E., Pilotto, A., Turrone, R., Cosseddu, M., Alberici, A., Paghera, B., Borroni, B., Padovani, A., Perani, D., 2017. Altered brain metabolic connectivity at multiscale level in early Parkinson's disease. Sci. Rep. 7, 4256. https://doi.org/10.1038/s41598-017-04102-z.

Schindlbeck, K.A., Lucas-Jiménez, O., Tang, C.C., Morbelli, S., Arnaldi, D., Pardini, M., Pagani, M., Ibarretxe-Bilbao, N., Ojeda, N., Nobili, F., Eidelberg, D., 2019. Metabolic network abnormalities in drug-naïve Parkinson's disease. Mov. Disord. mds.27960 https://doi.org/10.1002/mds.27960.

Spetsieris, P.G., Eidelberg, D., 2011. Scaled subprofile modeling of resting state imaging data in Parkinson's disease: methodological issues. Neuroimage 54, 2899–2914. https://doi.org/10.1016/j.neuroimage.2010.10.025.

Strafella, A.P., Bohnen, N.I., Perlmutter, J.S., Eidelberg, D., Pavese, N., Van Eimeren, T., Piccini, P., Politis, M., Thobois, S., Ceravolo, R., Higuchi, M., Kaasinen, V., Masellis, M., Peralta, M.C., Obeso, I., Pineda-Pardo, J.Á., Cilia, R., Ballanger, B., Niethammer, M., Stoessl, J.A., 2017. Molecular imaging to track Parkinson's disease and atypical parkinsonisms: new imaging frontiers. Mov. Disord. 32, 181–192. https://doi.org/10.1002/MDS.26907.

Tang, C.C., Poston, K.L., Dhawan, V., Eidelberg, D., 2011. Abnormalities in metabolic network activity precede the onset of motor symptoms in Parkinson's disease. J. Neurosci. 30, 1049–1056. https://doi.org/10.1523/JNEUROSCI.4188-09.2010.

Taylor, J.R., Elsworth, J.D., Roth, R.H., Sladek Jr., J.R., Redmond Jr., D.E., 1997. Severe long-term 1-methyl-4-phenyl-1,2,3,6-tetrahydropyridine-induced parkinsonism in the vervet monkey (Cercopithecus aethiops sabaeus). Neuroscience 81, 745–755.

Trigo-Damas, I., Del Rey, N.L.-G., Blesa, J., 2018. Novel models for Parkinson's disease and their impact on future drug discovery. Expert Opin. Drug Discovery 13, 229–239. https://doi.org/10.1080/17460441.2018.1428556.

Villalba, R.M., Lee, H., Smith, Y., 2009. Dopaminergic denervation and spine loss in the striatum of MPTP-treated monkeys. Exp. Neurol. 215, 220–227. https://doi.org/10.1016/j.expneurol.2008.09.025.

Xiang, X., Wind, K., Wiedemann, T., Blume, T., Shi, Y., Briel, N., Beyer, L., Biechele, G., Eckenweber, F., Zatcepin, A., Lammich, S., Ribicic, S., Tahirovic, S., Willem, M., Deussing, M., Palleis, C., Rauchmann, B.S., Gildehaus, F.J., Lindner, S., Spitz, C., Franzmeier, N., Baumann, K., Rominger, A., Bartenstein, P., Ziegler, S., Drzezga, A., Respondek, G., Buerger, K., Perneczky, R., Levin, J., Höglinger, G.U., Herms, J., Haass, C., Brendel, M., 2021. Microglial activation states drive glucose uptake and FDG-PET alterations in neurodegenerative diseases. Sci. Transl. Med. 13 https://doi.org/10.1126/SCITRANSLMED.ABE5640.

Zeighami, Y., Ulla, M., Iturria-Medina, Y., Dadar, M., Zhang, Y., Larcher, K.M.-H., Fonov, V., Evans, A.C., Collins, D.L., Dagher, A., 2015. Network structure of brain atrophy in de novo Parkinson's disease. Elife 4. https://doi.org/10.7554/eLife.08440.